Hindawi
Mathematical Problems in Engineering
Volume 2017, Article ID 6510213, 12 pages
https://doi.org/10.1155/2017/6510213

Research Article

Spinning Reserve Requirements Optimization Based on an Improved Multiscenario Risk Analysis Method

Liudong Zhang,[1,2] Yubo Yuan,[1] Xiaodong Yuan,[1] Bing Chen,[1] Dawei Su,[3] and Qiang Li[1]

[1]*Electric Power Research Institute, State Grid Jiangsu Electric Power Company, Nanjing, Jiangsu 211103, China*
[2]*School of Electrical Engineering, Southeast University, Nanjing, Jiangsu 210096, China*
[3]*Electric Power Dispatch and Control Center, State Grid Jiangsu Electric Power Company, Nanjing, Jiangsu 210024, China*

Correspondence should be addressed to Liudong Zhang; zldon_1987@126.com

Received 9 October 2016; Revised 20 February 2017; Accepted 27 February 2017; Published 15 March 2017

Academic Editor: Paolo Crippa

This paper proposes a novel security-constrained unit commitment model to calculate the optimal spinning reserve (SR) amount. The model combines cost-benefit analysis with an improved multiscenario risk analysis method capable of considering various uncertainties, including load and wind power forecast errors as well as forced outages of generators. In this model, cost-benefit analysis is utilized to simultaneously minimize the operation cost of conventional generators, the expected cost of load shedding, the penalty cost of wind power spillage, and the carbon emission cost. It remedies the defects of the deterministic and probabilistic methods of SR calculation. In cases where load and wind power generation are negatively correlated, this model based on multistep modeling of net demand can consider the wind power curtailment to maximize the overall economic efficiency of system operation so that the optimal economic values of wind power and SR are achieved. In addition, the impact of the nonnormal probability distributions of wind power forecast error on SR optimization can be taken into account. Using mixed integer linear programming method, simulation studies on a modified IEEE 26-generator reliability test system connected to a wind farm are performed to confirm the effectiveness and advantage of the proposed model.

1. Introduction

Wind power generation has been used in many countries as the most promising sustainable energy source to reduce the consumption of fossil fuels and curb emissions of carbon dioxide. However, because of the stochastic volatility and limited predictability of wind speed, power system operations are significantly challenged by the large-scale wind power integration. The influences include power quality, operating reserve, transient stability, and frequency and voltage control [1, 2]. In particular, the traditional unit commitment (UC) with deterministic spinning reserve (SR) requirements cannot adequately cope with uncertain wind power generation. Additional SR needs to be provided to ensure operational reliability [3, 4]. Therefore, various new methods taking into account wind power uncertainty in [5–20] have been presented to determine SR requirements. These methods can mainly be divided into three types:

(i) The deterministic methods [5–9]: in [5–9], the minimum amount of SR is set to be the largest capacity of online generators, or some proportion of the standard deviation of the net demand or wind power forecast error, or their combination. Although these deterministic methods are easy to implement, they are inadequate in dealing with the stochastic nature of various uncertainties in power systems and the economic efficiency of system operation.

(ii) The probabilistic methods [10–13]: in the reliability-constrained UC [10, 11, 13] and method [12], probabilistic reliability criteria that are defined by the loss of load probability (LOLP) or the expected energy not

served (EENS) implicitly determine the SR requirements. In each time period, the probabilistic method can ensure that the system will maintain a specified reliability level under which the optimal economic efficiency of system operation can be achieved. However, this method neglects the setting of the reliability metrics and the rationality of such metrics.

(iii) The methods based on cost-benefit analysis [14–20]: by introducing the notion of value of lost load (VOLL), the optimization of the SR requirements based on cost-benefit analysis conducts an economic value analysis for the cost and benefit of providing SR so as to achieve a tradeoff between economics and reliability. Thus, the experiential settings of the required SR amount [5–9] and reliability metrics [10–13] are avoided.

It is well known that wind power generation needs to be controlled by "spilling wind" owing to the transmission congestion. Due to the fact that there is no fuel consumption in wind power generation, wind power spillage, which is also called "wind power curtailment," increases the load supplied by conventional generators and thereby increases the fuel cost and emission cost of these generators. On the other hand, in cases where load and wind power generation are negatively correlated, wind power spillage will diminish the peak-valley difference of net demand so that the start-up and shutdown costs of peaking generators can be reduced [5]. Moreover, wind power spillage reduces the underestimation of wind power output, which may decrease the system EENS and thus reduce additional SR amount. Therefore, besides security issues, these two conflicting and opposite effects of wind power spillage should be considered while optimizing SR requirements from the overall economic and low-carbon efficiency of system operation.

The UC in [5, 6, 14–18] comprehensively consider the effects of wind power spillage on the total cost of system operation and SR quantification. Nevertheless, these studies have other various limitations in system EENS calculation. The following are specifically mentioned.

(i) Modeling: a stochastic planning method based on a scenario tree is adopted in [14–16] to simulate the probability distribution of forecast errors of net demand or wind power so that the EENS of every scenario can be determined. However, the forced outage rates (FOR) of generators are not taken into account, which may lead to an underestimation of SR. Similarly, Lee [17] used a capacity outage probability table to calculate the system EENS based on the simplified assumptions of wind power and load forecast errors.

(ii) Optimization process: Ortega-Vazquez [18] considered the load and wind power forecast errors as well as FOR of generators in determining the optimal SR amount for each time period. In reserve-constrained UC, these SR requirements are then set as constraints. However, based on a time-decoupled UC problem, the preprocessing may result in a suboptimal solution.

The aforementioned conservative methods [14–18] can be improved by using a multiscenario risk analysis method [20] that is capable of taking into account the probabilistic distribution of load and wind power forecast errors, as well as FOR of generators. However, wind power spillage and the nonnormal probability distributions of load and wind power forecast errors cannot be taken into account in the system EENS calculation in [20]. This may affect the optimal determination of SR requirements.

Therefore, based on [20] and by combining cost-benefit analysis with an improved multiscenario risk analysis method, this paper proposes a novel security-constrained unit commitment (SCUC) model to determine the optimal SR amount. Specifically, in order to consider wind power spillage and the nonnormal probability distribution of wind power forecast error in system EENS calculation, the single discretization of net demand forecast error in [20] is extended into the respective discretization of wind power and load forecast errors. After the EENS under each scenario is calculated, the system EENS can be determined by probability-weighted aggregation. The proposed UC model can be formulated as mixed integer linear programming (MILP) and solved with a commercial solver like CPLEX to improve the computational efficiency and robustness.

The contributions and added value of this paper compared with the respective cited methods are threefold: (1) an improved multiscenario risk analysis method capable of considering various uncertainties including load and wind power forecast errors as well as forced outages of generators is proposed to optimize the spinning reserve requirements; (2) compared with the respective cited methods including the deterministic methods [5–9] and probabilistic methods [10–13] as well as the cost-benefit analysis [14–20], the proposed method can consider the impacts of various uncertainties including the nonnormal probability distributions and curtailments of wind power on the overall economic efficiency of system operation via combining cost-benefit analysis with the proposed improved multiscenario risk analysis method so that the optimal economic values of wind power and SR are achieved; (3) the proposed UC model is formulated as a MILP which can be solved effectively via commercial solvers. However, it should be noted that the practical limitation of the proposed method is its computational efficiency. Because of the huge number of decision variables caused by various uncertainties including forecast errors of load and wind power as well as FOR of generators, the simulation times of [20] and the proposed method are larger than the ones of the deterministic methods and probabilistic methods. Hence, the method in [20] and the proposed method are not suitable for online applications of a large-scale power system.

The remainder of this paper is laid out as follows. First of all, Section 2 presents the procedure of improved

EENS calculation method with consideration of wind power spillage and the nonnormal probability distribution of wind power forecast error. Then, the SCUC model is proposed in Section 3. After that, in Section 4, the case studies and simulation results analysis are presented. At last, in Section 5, main conclusions are summarized.

2. Formulation of EENS

In this section, based on multistep modeling of net demand, an improved multiscenario risk analysis method capable of taking into account different probability distributions of the load and wind power forecast errors, as well as FOR of generators, is proposed to determine the system EENS with consideration of wind power spillage. The formulation of EENS is later transformed into an equivalent MILP form.

2.1. Improved EENS Calculation Method with Consideration of Wind Power Spillage. The system EENS is caused by the available SR not being able to meet the excess of load and wind power forecast errors plus shortfalls in the power output of online generators [20]. In this paper, the unit of EENS is MWh.

In [20], the generator outages are a series of binary variables, whereas the net demand forecast error is a continuous variable. In general, the EENS formulation can be divided into three steps.

Step 1. Based on "$N-1$" or "$N-2$" contingency rules, a scenario set is constructed.

Step 2. The normal distribution of net demand forecast error is discretized into NL (NL = 7) intervals and then combined with the contingency events in each scenario.

Step 3. By summing the expectations of NL intervals resulting in some loss of load, the EENS in a scenario is determined. The total system EENS is the summation of all EENS of each scenario weighted by probabilities of corresponding scenarios.

Unlike [20], wind power spillage and the nonnormal distribution of load and wind power forecast errors are considered in the system EENS calculation of the proposed method. The method in [20] is unable to combine wind power spillage with net demand forecast error and deal with different probability distributions. Consequently, the single discretization of net demand forecast error in Step 2 of [20] needs to be extended into the respective discretization of wind power and load forecast errors. Therefore, the three steps in [20] are extended into four steps in the proposed method as shown in Figure 1.

In Step 1, only single-outage random events are considered, because multiple-outage random events have relatively small probabilities in the scheduling horizon while consuming far more computational resources. In addition, the probability distribution of wind power and load forecast errors in Steps 2 and 3 can be divided into smaller intervals. Though higher accuracy of the result can be achieved with small intervals, more computational resources will be required.

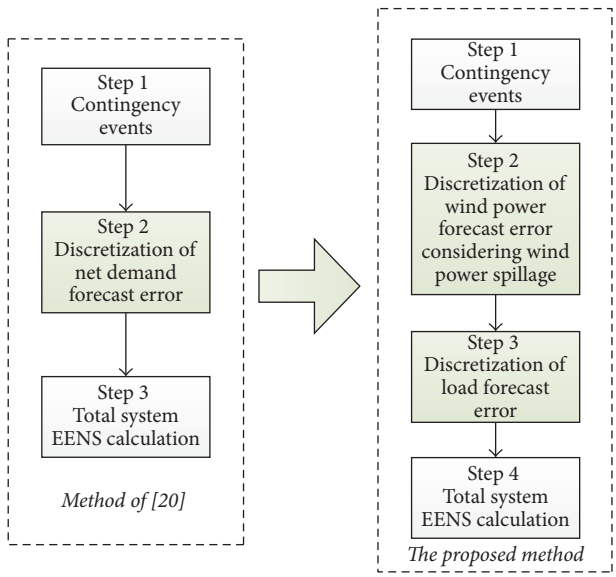

Figure 1: Comparison of EENS calculation process between the method of [20] and the proposed method.

2.2. Procedure of Improved EENS Calculation Method with Consideration of Wind Power Spillage and the Nonnormal Probability Distribution. The improved EENS calculation process with consideration of wind power spillage and the nonnormal probability distribution can be described as follows.

Step 1. Note that the random outage events among NI generators are independent of each other. The probability P_i^t of all scheduled generators available except generator i is

$$P_i^t = u_i^t U_i \prod_{j=1, j\neq i}^{\mathrm{NI}} \left(1 - u_j^t U_j\right) \approx u_i^t U_i. \tag{1}$$

NI + 1 fault scenarios can be constructed according to no contingency event and single-order contingency events. During period t, taking scenario s as an example, the deficient or redundant SR amount μ_s^t of other generators in accordance with the outage generator i under scenario s can be calculated as

$$\mu_s^t = \sum_{j=1}^{\mathrm{NI}} r_j^t - \left(p_i^t + r_i^t\right). \tag{2}$$

Note that the scenario of no contingency event is the base scenario, when $s = 0$.

Step 2. Wind power forecast error is considered to follow a nonnormal distribution in [21, 22], similar to load forecast error. But, for the convenience of description and without loss of generality, the normal distribution is still chosen as an example in this paper. The normal distribution of wind

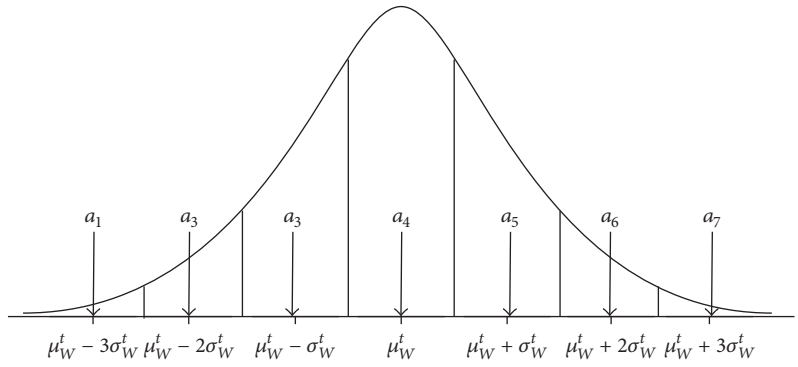

Figure 2: Seven-interval discretization of normal distribution of wind power forecast error.

power forecast error is approximately discretized into NL (NL = 7) intervals. Figure 2 shows typical seven-interval discretization of wind power forecast error modeled as a continuous normally distributed random variable with zero mean μ_W^t and a standard deviation σ_W^t. The probability of interval l_1 is θ_{l_1}, and the width of each interval is σ_W^t. For each interval l_1 ($l_1 = 1, 2, \ldots, 7$), the midvalue $a_{l_1} = \mu_W^t + (l_1 - (\mathrm{NL}+1)/2)\sigma_W^t$ represents the value of corresponding whole interval. Figure 2 shows typical seven-interval discretization of continuous normal distribution of wind power forecast error.

Combining the realization of uncertainties of generators in fault scenarios with NL intervals of wind power forecast error, (NI + 1) × NL new scenarios can be constructed. Then, after adding a_{l_1} to μ_s^t, the system forecast error μ_{s,l_1}^t caused by the uncertainties of generators and wind power forecast error can be formulated as

$$\mu_{s,l_1}^t = \begin{cases} \mu_s^t + \lambda_{l_1}^t \left[\left(l_1 - \dfrac{(\mathrm{NL}+1)}{2} \right) \sigma_W^t + s_W^t \right], & l_1 \in [1,4] \\ \mu_s^t + \left(l_1 - \dfrac{(\mathrm{NL}+1)}{2} \right) \sigma_W^t, & l_1 \in [5, \mathrm{NL}]. \end{cases} \tag{3}$$

In (3), a binary variable $\lambda_{l_1}^t$ is introduced to judge whether s_W^t has effects on the value of wind power forecast error $(l_1 - (\mathrm{NL}+1)/2)\sigma_W^t$ ($l_1 \le 4$). When $l_1 \ge 5$, wind power spillage has no effect on the overestimation of wind power output. The binary variable $\lambda_{l_1}^t$ ($l_1 \le 4$) satisfies

$$\lambda_{l_1}^t = \begin{cases} 1, & \text{if } \left(l_1 - \dfrac{(\mathrm{NL}+1)}{2} \right) \sigma_W^t + s_W^t < 0 \\ 0, & \text{otherwise.} \end{cases} \tag{4}$$

The nonlinear conditional expression in (4) can be equivalent to the following linear inequalities:

$$-\frac{\left[(l_1 - (\mathrm{NL}+1)/2)\, \sigma_W^t + s_W^t \right]}{\sum_{i=1}^{\mathrm{NI}} p_i^{\max}} \le \lambda_{l_1}^t \le 1 - \frac{\left[(l_1 - (\mathrm{NL}+1)/2)\, \sigma_W^t + s_W^t \right]}{\sum_{i=1}^{\mathrm{NI}} p_i^{\max}}. \tag{5}$$

Step 3. Load forecast error is similarly modeled as a normally distributed random variable with zero mean μ_L^t and a standard deviation σ_L^t. The probability distribution of load forecast error can be similarly discretized into NL intervals, and the probability of interval l_2 is denoted as θ_{l_2}. In each interval l_2, μ_{s,l_1}^t is subtracted from $(l_2 - (\mathrm{NL}+1)/2)\sigma_L^t$ to calculate the total system forecast error. The intervals only need to satisfy

$$\left(l_2 - \frac{(\mathrm{NL}+1)}{2} \right) \sigma_L^t - \mu_{s,l_1}^t > 0. \tag{6}$$

In order to differentiate the intervals satisfying (6) from others, it is necessary to introduce another new binary variable b_{s,l_1,l_2}^t which satisfies

$$b_{s,l_1,l_2}^t = \begin{cases} 1, & \text{if } \left(l_2 - (\mathrm{NL}+1)/2 \right) \sigma_L^t - \mu_{s,l_1}^t > 0 \\ 0, & \text{otherwise.} \end{cases} \tag{7}$$

The nonlinear formulation above can be linearized to

$$\frac{\left[(l_2 - (\mathrm{NL}+1)/2)\, \sigma_L^t - \mu_{s,l_1}^t \right]}{\sum_{i=1}^{\mathrm{NI}} p_i^{\max}} \le b_{s,l_1,l_2}^t \le 1 + \frac{\left[(l_2 - (\mathrm{NL}+1)/2)\, \sigma_L^t - \mu_{s,l_1}^t \right]}{\sum_{i=1}^{\mathrm{NI}} p_i^{\max}}, \tag{8}$$

Step 4. During period t, the EENS in each scenario constructed in Step 2 can be determined by summing the expectations of all intervals causing some loss of load as expressed in

$$\mathrm{EENS}_{s,l_1}^t = \sum_{l_2=1}^{\mathrm{NL}} \left[\left(l_2 - \frac{\mathrm{NL}+1}{2} \right) \sigma_L^t - \mu_{s,l_1}^t \right] \theta_{l_2} b_{s,l_1,l_2}^t. \tag{9}$$

Then, during period t, the total system EENS is the summation of EENS_{s,l_1}^t weighted by probabilities of corresponding scenarios

$$\mathrm{EENS}^t = \sum_{s=0}^{\mathrm{NI}} \sum_{l_1=1}^{\mathrm{NL}} \mathrm{EENS}_{s,l_1}^t \theta_{l_1} P_s^t. \tag{10}$$

It is worth noting that when the assumptive normal distribution of wind power forecast error is not correct, the aforementioned EENS calculation method will still be valid. By discretizing the new probability distribution of wind power forecast error into several intervals in Step 2, a_{l_1} in (3), (4), and (5) and θ_{l_1} in (10) can be replaced by the values of wind power forecast error and probability in each interval, respectively. In the same way, the load forecast error which follows the nonnormal distribution can be similarly treated.

2.3. EENS Linearization. In (10), EENS^t are formulated as the sum of products of a continuous variable and three binary variables. According to the linearization method in [23], EENS^t can be transformed into a series of linear inequalities.

The linearization process can be described as follows.

Step 1. A binary variable y^t_{s,l_1,l_2} and a continuous variable s^t_{W,l_1} are introduced. Let y^t_{s,l_1,l_2} be the product of the binary variable b^t_{s,l_1,l_2} and the binary variable u^t_i, and let s^t_{W,l_1} be the product of the bounded continuous variable s^t_W and the binary variable $\lambda^t_{l_1}$. Then, EENS^t will be transformed into the summation of products of a binary variable and a continuous variable. The above new variables y^t_{s,l_1,l_2} and s^t_{W,l_1} can be equivalent to the following linear constraints:

$$\begin{aligned} 0 &\le y^t_{s,l_1,l_2} \le b^t_{s,l_1,l_2} \\ y^t_{s,l_1,l_2} &\le u^t_i \\ y^t_{s,l_1,l_2} &\ge b^t_{s,l_1,l_2} + u^t_i - 1 \end{aligned} \tag{11}$$

$$\begin{aligned} -\lambda^t_{l_1} W^t_f \le s^t_{W,l_1} &\le \lambda^t_{l_1} W^t_f \\ s^t_{W,l_1} &\le s^t_W + \left(1 - \lambda^t_{l_1}\right) W^t_f \\ s^t_{W,l_1} &\ge s^t_W - \left(1 - \lambda^t_{l_1}\right) W^t_f. \end{aligned} \tag{12}$$

Step 2. Let $\text{EENS}^t = \sum_{s=0}^{\text{NI}} \sum_{l_1=1}^{\text{NL}} \sum_{l_2=1}^{\text{NL}} E^t_{s,l_1,l_2}$, and E^t_{s,l_1,l_2} can be formulated as

$$E^t_{s,l_1,l_2} = \left[\left(l_2 - \frac{(\text{NL}+1)}{2}\right)\sigma^t_L - \mu^t_{s,l_1}\right]\theta_{l_1}\theta_{l_2} y^t_{s,l_1,l_2} U_i, \tag{13}$$

where $\mu^t_{s,l_1} = \sum_{j=1}^{\text{NI}} r^t_j - r^t_i - p^t_i + \lambda^t_{l_1}(l_1 - (\text{NL}+1)/2)\sigma^t_W + s^t_{W,l_1}$ when $l_1 \in [1,4]$. It can be observed from (13) that E^t_{s,l_1,l_2} is a nonlinear formulation consisting of the product of a bounded continuous variable and a binary variable, which can be equivalent to the following linear constraints:

$$\begin{aligned} &-U_i\theta_{l_1}\theta_{l_2} y^t_{s,l_1,l_2} \sum_{j=1}^{\text{NI}} p^{\max}_j \le E^t_{s,l_1,l_2} \\ &\quad \le U_i\theta_{l_1}\theta_{l_2} y^t_{s,l_1,l_2}\left[p^{\max}_i + 3\left(\sigma^t_L + \sigma^t_W\right)\right] \\ &E^t_{s,l_1,l_2} \\ &\quad \le U_i\theta_{l_1}\theta_{l_2}\left[\left(l_2 - \frac{\text{NL}+1}{2}\right)\sigma^t_L - \mu^t_{s,l_1}\right] \\ &\qquad + U_i\theta_{l_1}\theta_{l_2}\left(1 - y^t_{s,l_1,l_2}\right)\sum_{j=1}^{\text{NI}} p^{\max}_j \\ &E^t_{s,l_1,l_2} \\ &\quad \ge U_i\theta_{l_1}\theta_{l_2}\left[\left(l_2 - \frac{\text{NL}+1}{2}\right)\sigma^t_L - \mu^t_{s,l_1}\right] \\ &\qquad - U_i\theta_{l_1}\theta_{l_2}\left(1 - y^t_{s,l_1,l_2}\right)\left[p^{\max}_i + 3\left(\sigma^t_L + \sigma^t_W\right)\right]. \end{aligned} \tag{14}$$

3. Problem Formulation of SCUC Based on Cost-Benefit Analysis

In this section, the mathematical formulation of the SCUC problem is presented. The expected cost of load shedding (ECLS) is expressed as the approximation of EENS given in Section 2 multiplied by VOLL and then added to the objective function of the proposed SCUC model so that the optimal wind power spillage and the optimal quantification of SR are achieved.

3.1. Objective Function. The objective function of conventional UC usually only considers the generation cost (GC) of conventional generators over all scheduling periods. This generation cost contains the fuel cost, start-up cost, and SR cost of generators. However, in the proposed formulation based on cost-benefit analysis, the SR requirements are determined by minimizing the sum of generation cost of generators and ECLS. In addition, though wind power spillage results in additional fuel cost and carbon emission cost (CC) of conventional generators, the penalty cost (PC) of wind power spillage is still considered in the objective function from the wind power's priority in scheduling policy and other environmental benefits of it. Thus, the objective function of the proposed SCUC is defined as

$$\min\left\{\sum_{t=1}^{\text{NT}}\left(\text{GC}^t + \text{ECLS}^t + \text{CC}^t + \text{PC}^t\right)\right\}. \tag{15}$$

3.1.1. Generation Cost of Conventional Generators. The generation cost consists of the start-up cost, fuel cost, and SR cost of conventional generators, which is calculated by

$$\text{GC}^t = \sum_{i=1}^{\text{NI}}\left(c_i\left(u^t_i, p^t_i\right) + c_{\text{su},i} u^t_i\left(1 - u^{t-1}_i\right) + c_{r,i} r^t_i\right), \tag{16}$$

where $c_i(u_i^t, p_i^t)$ is the fuel cost of generator i during period t which is described by the consumption characteristic curve of a quadratic function; $c_{\mathrm{su},i}u_i^t(1-u_i^{t-1})$ is the start-up cost of generator i during period t; $c_{r,i}r_i^t$ is the reserve cost of generator i to supply SR amount r_i^t during period t.

3.1.2. ECLS. Here,

$$\mathrm{ECLS}^t = \mathrm{EENS}^t \times \mathrm{VOLL}, \tag{17}$$

where VOLL is the generator outage loss value for users, that is, the loss for outage of 1 MWh electricity, usually estimated via consumer survey [24].

3.1.3. Carbon Emission Cost of Conventional Generators. In this paper, it is supposed that Clean Development Mechanism (CDM) in Kyoto Protocol [25] is the carbon trading mechanism employed. The carbon emission cost during period t CC^t can be calculated by

$$\mathrm{CC}^t = K_{\mathrm{CDM}}\left(M_C^t - M_D^t\right). \tag{18}$$

The calculation of carbon emission cost (18) can be divided into two cases:

(i) When $M_C^t > M_D^t$, the carbon emission of power systems exceeds the credit and $M_C^t - M_D^t$ is the excessive part. Supplementary carbon emission allowance obtained by CDM is then required, thereby increasing the cost for system operation.

(ii) When $M_C^t \le M_D^t$, the carbon emission of power systems is lower than the credit; that is, there is surplus which can be sold through emission transaction and the system operation cost is then decreased equivalently.

The total carbon emission M_C^t during period t is commonly calculated by

$$M_C^t = \sum_{i=1}^{\mathrm{NI}}\left[\alpha_i\left(p_i^t\right)^2 + \beta_i p_i^t + \gamma_i + \xi_i e^{\lambda_i p_i^t}\right]. \tag{19}$$

Because (19) is too complex for calculation, it can be replaced by the following equation given in [25]:

$$M_C^t = \sum_{i=1}^{\mathrm{NI}}\left\{\frac{F_{c,i}\left[c_i\left(u_i^t, p_i^t\right) + c_{\mathrm{su},i}u_i^t\left(1-u_i^{t-1}\right)\right]}{K_F}\right\}, \tag{20}$$

where the unit of $F_{c,i}$ is $\mathrm{tCO_2}$/tce where tce refers to the ton of standard coal equivalent.

The carbon emission credit M_D^t during period t and the total carbon emission credit M_D of power systems are determined by the load of each period; that is,

$$M_D^t = \frac{\left(M_D L_f^t\right)}{\sum_{t=1}^{T} L_f^t}. \tag{21}$$

3.1.4. Penalty Cost of Wind Power Spillage. The penalty cost of wind power spillage during period t PC^t is calculated by

$$\mathrm{PC}^t = V_S s_W^t. \tag{22}$$

3.2. Constraint Conditions

3.2.1. Power Balance Constraint. One has

$$L_f^t - W_f^t + s_W^t - \sum_{i=1}^{\mathrm{NI}} u_i^t p_i^t = 0, \tag{23}$$

where s_W^t satisfies $0 \le s_W^t \le W_f^t$.

3.2.2. SR Constraints of Generators. Here, one has

$$0 \le r_i^t \le \min\left(u_i^t p_i^{\max} - u_i^t p_i^t, T_{10} r_u^i\right), \tag{24}$$

where $T_{10}r_u^i$ is the maximum 10-minute SR supplied by generator i [17].

3.2.3. Upper and the Lower Limits for the Power Output of Generators. One has

$$u_i^t p_i^{\min} \le p_i^t \le u_i^t p_i^{\max}. \tag{25}$$

3.2.4. Ramp-Rate Limits of Generators. One has

$$-r_d^i \le p_i^t - p_i^{t-1} \le r_u^i. \tag{26}$$

3.2.5. Minimum Up- and Down-Time Constraints of Generators. One has

$$\begin{aligned}\left(u_i^{t-1} - u_i^t\right)\left(T_{i,t-1}^{\mathrm{on}} - T_{i,\min}^{\mathrm{on}}\right) &\ge 0\\ \left(u_i^t - u_i^{t-1}\right)\left(T_{i,t-1}^{\mathrm{off}} - T_{i,\min}^{\mathrm{off}}\right) &\ge 0.\end{aligned} \tag{27}$$

3.2.6. Transmission Flow Limits Modeled by Direct Current Power Flow. One has

$$\begin{aligned}p_{g,k}^t + \left(p_{w,k}^t - p_{\mathrm{sw},k}^t\right) - p_{d,k}^t &= \sum_j \frac{\left(\delta_j^t - \delta_k^t\right)}{X_{kj}}\\ -p_{kj}^{\max} \le \frac{\left(\delta_j^t - \delta_k^t\right)}{X_{kj}} &\le p_{kj}^{\max}.\end{aligned} \tag{28}$$

3.2.7. Carbon Trading Constraint. Due to the restrictions of financial and technical levels, the carbon emission reduction by CDM has an upper bound expressed by

$$\left|M_C^t - M_D^t\right| \le \left|M_C^t - M_D^t\right|_{\max}. \tag{29}$$

3.3. UC Problem Solution. UC is a large-scale, nonlinear, nonconvex, mixed integer programming problem with a large number of discrete and continuous variables. At present, various methods have been proposed for its solution: from

the early complete enumeration, priority list method, and dynamic programming to the current branch-and-bound method and intelligent optimization algorithm in [8, 17]. In recent years, the commercial software CPLEX has utilized branch-cutting on the basis of branch-and-bound method and combined various techniques, such as the heuristic method and cutting-plane algorithm, to solve the MILP problem. So far, CPLEX has been widely used to solve UC problems in [5, 7, 14–16, 18–20] by approximately linearizing the UC problem to a MILP model. Therefore, this paper also adopts this solver for the solution of the proposed SCUC problem where the operation cost in objective function given by (15) and constraints (23)–(29) are linearized in accordance with the method proposed in [18] which is presented in the Appendix.

The deterministic methods and probabilistic methods are incomplete without the inclusion of a discussion on the impact of FOR. From a computational point of view, the addition of generator contingencies would render the solution process of the UC problem of [20] and the proposed UC problem much more challenging. The addition of a single generator contingency, also considering its possible times of failure, would multiply the number of scenarios by the number of periods of the scheduling horizon. It can be recalled that, with each extra scenario, there are corresponding extra variables and constraints. As a result, realistically sized problems such as the European interconnected power system may be very hard to handle with current computing tools in a reasonable amount of time required for day-ahead UC. However, some modeling simplifications could be considered. One possibility is to make use of the scenario reduction techniques [26]. Secondly, decomposition techniques [27] are promising because they exploit the intrinsic decomposable structure of the problem whereby each scenario is optimized individually under the command of a master coordinating problem. These aspects need to be further investigated in subsequent researches.

4. Case Studies and Simulation Results Analysis

The proposed method for determining SR in this section is tested and verified on a modified IEEE 26-generator reliability test system. Simulation studies are carried out to draw comparisons of UC results between the proposed method and method of [20] to verify the effectiveness and advantage of the proposed SCUC model.

4.1. Modified IEEE 26-Generator Reliability Test System. A modified IEEE 26-generator reliability test system is adopted in this paper to verify the effectiveness of the proposed model. In this system, there are 26 thermal generators with a total capacity of 3105 MW. The hydro generating units have been omitted. The transmission limits, failure rates, ramp rates, cost coefficients, and minimum up and down time are obtained from [18, 28]. The power output of the generators committed at $t = 0$ is obtained by the economic dispatch of the committed generators at a load level of 1840 MW. One wind farm is added at bus 14. Its capacity is set at 800 MW, 25.7% of the total conventional generation capacity. To illustrate the effect of wind power spillage on the determination of SR requirements, Table 1 lists the forecast load and power output of wind farm used for testing. It can be observed from the table that the wind power output and load are negatively correlated. The standard deviations of load and wind power forecast error can be approximately calculated according to [18]. VOLL is set at 4000 \$/MWh [20]. V_S is set at 10 \$/MWh. The CDM transaction price K_{CDM} is 50 \$/tCO_2, $F_{c,i}$ is 3 tCO_2/tce, and K_F is 100 \$/tce [25]. Considering the effects of maximizing carbon emission cost on SR optimization, the carbon emission credit M_D^T is set at 0.

Table 1: Forecast data of load and power output of wind farm.

Hour	Load (MW)	Power output of wind farm (p.u.)
1	1700	0.845
2	1730	0.928
3	1690	0.923
4	1700	0.853
5	1750	0.820
6	1850	0.715
7	2000	0.498
8	2430	0.424
9	2540	0.338
10	2600	0.370
11	2670	0.193
12	2590	0.386
13	2390	0.597
14	2050	0.696
15	1820	0.810
16	1750	0.956
17	1700	0.895
18	1730	0.693
19	1860	0.583
20	2150	0.468
21	2400	0.391
22	2480	0.276
23	2200	0.562
24	1840	0.752

The proposed model is solved on a 2.66 GHz Windows-based workstation with 8 GB of RAM using a MILP solver CPLEX 12.5 under MATLAB environment. When the duality gap tolerance for CPLEX solver is set at 0.5%, the computation time is about 11.2 s.

4.2. Comparison of the Proposed Method and the Method of [20]

4.2.1. Necessity Analysis with Consideration of Wind Power Spillage. Wind power has been given priority in scheduling. However, the development of Chinese power grid in regions with abundant wind energy resources (Xinjiang, Ningxia,

Table 2: Comparison of different costs between the proposed method and the method presented in [20].

Cost	The proposed method	Method in [20]
Fuel cost ($)	228721.81	227545.48
Start-up cost ($)	4929.00	6150.60
SR cost ($)	58185.61	62022.23
ECLS ($)	15779.94	15960.19
Penalty cost ($)	856.5	0
Carbon emission cost ($)	195433.41	193470.31
Total cost ($)	503906.28	505148.81

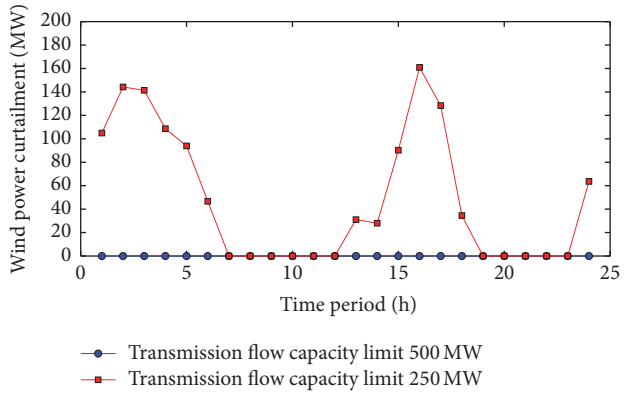

Figure 3: Wind power curtailments with different capacity limits of transmission lines.

Gansu, etc.) is far behind the increase of installed wind power capacity at present, and thereby the large-scale wind power accommodation capacity of power systems is insufficient. Wind power spillage must be adopted to ensure the security and stability of systems operation.

When the capacity limit 500 MW of the transmission lines between buses 14 and 11 and 14 and 16 is modified to 250 MW in the test system, it can be seen from Figure 3 that the transmission flow capacity is insufficient and thereby the wind power cannot be completely accommodated in the proposed method. At this time, the network security constraints in [20] which has no solution are not satisfied. This verifies the necessity of utilizing multistep modeling of net demand to improve the traditional multiscenario risk analysis method of SR optimization.

4.2.2. Economic Analysis with Consideration of Wind Power Spillage. Compared with the method presented in [20], wind power spillage is taken into account. Table 2 compares different costs (fuel cost, start-up cost, SR cost, ECLS, penalty cost, carbon emission cost, and total cost) between the proposed method and the method of [20] over the whole time periods. It can be observed from this table that although the fuel cost of conventional generators, the penalty cost, and the carbon emission cost increase when wind power spillage is considered, reductions in ECLS, SR cost, start-up cost, and total cost are achieved. Therefore, the optimal determination

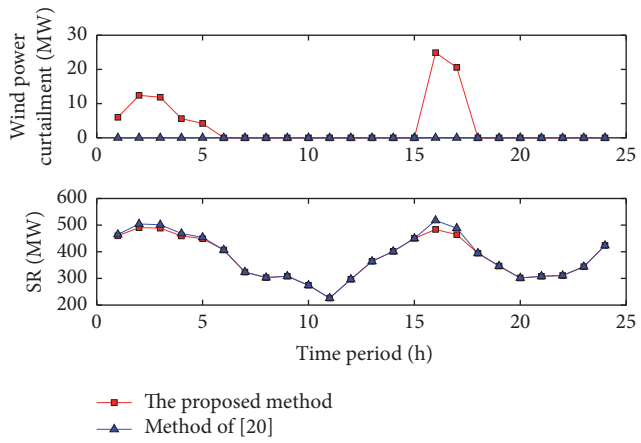

Figure 4: Comparison of wind power curtailments and SR between the proposed method and the method in [20].

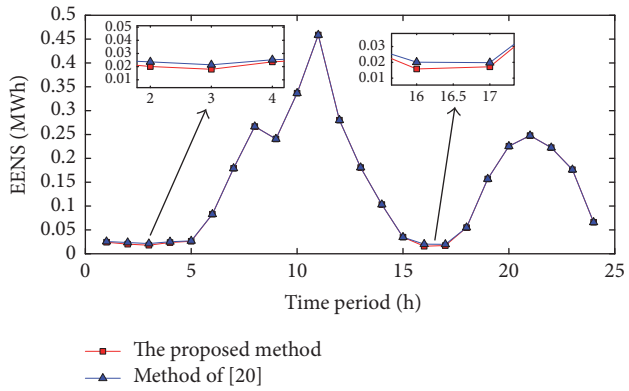

Figure 5: Comparison of EENS between the proposed method and the method of [20].

of SR requirements and the optimal economic value of wind power are realized. This verifies the advantage of the proposed model. The lower total cost of the proposed method can be explained in detail as in Table 2.

Firstly, Figure 3 shows the variation of wind power spillage during all periods in the proposed method. Figures 4 and 5 compare the SR and EENS, respectively, between the proposed method and the method of [20].

(i) When the load level is low and wind power output is large during periods 1–5, 16, and 17, the amount of wind power spillage is not equal to zero. This is because the cost of providing additional SR is higher than the sum of increased fuel cost of conventional generators, the penalty cost, and the carbon emission cost caused by wind power spillage during these periods. Consequently, by increasing a small amount of wind power spillage, the amount of SR is reduced and the system EENS is reduced simultaneously.

Take periods 3 and 16 as an example. On the one hand, this method curtails wind power values 11.87 MW and 24.89 MW, respectively, which leads to the penalty

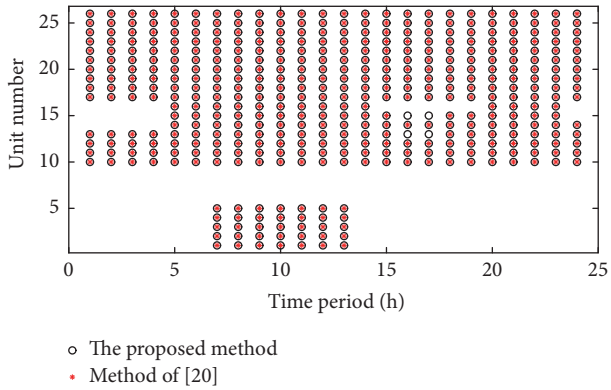

Figure 6: Comparison of the generation schedules between the proposed method and the method of [20].

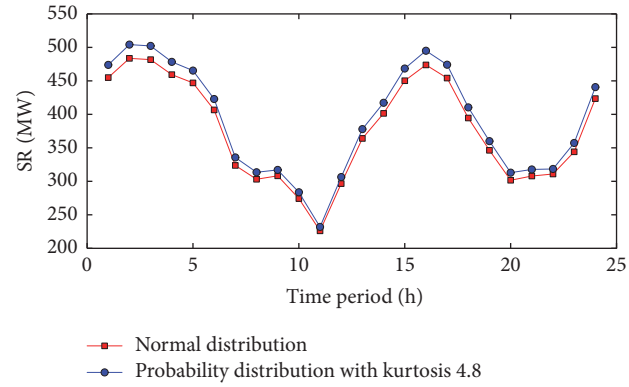

Figure 7: Comparison of SR between different probability distributions.

cost increase by 118.70$ and 248.90$, respectively, and the carbon emission cost increase by 256.40$ and 575.70$, respectively, as well as the fuel cost of conventional generators increase by 152.62$ and 353.37$, respectively. On the other hand, the SR cost decreases by 539.23$ and 1109.52$, respectively, and ECLS decreases by 30.06$ and 55.37$, respectively. In summary, during period 3, the total scheduling cost can reduce by 41.57$. During period 16, the amount of wind power spillage is larger, and the sum of these costs increases by 13.08$ caused by wind power spillage. However, Figure 6 compares the generation schedules between the two methods. It can be seen from this figure that when the system load level is low during periods 16 and 17, the outages of generators 13 and 15 are avoided in the proposed method due to additional wind power curtailments. Consequently, the start-up cost of generators during the next period can be reduced (see the comparison of start-up cost shown in Table 2) and the overall economic efficiency of system operation will be improved.

(ii) When the load level is high and wind power output is small during other periods, more expensive generators are committed. As a result, the sum of increased fuel cost and the penalty cost caused by wind power spillage is higher than the cost of providing additional SR. Hence, the wind power will be completely accommodated during high load levels.

4.2.3. Simulation Analysis considering Different Probability Distributions of Wind Power Forecast Error. The study in [21] shows that the tail of the actual day-ahead wind power forecast error data curve is situated between the Laplace distribution and the normal distribution curve. Kurtosis is chosen as the statistical parameter to evaluate the tail of the studied probability density function, and the kurtosis of the actual wind power forecast error ranges from 3 to 6. Therefore, in this paper, the kurtosis value of the new wind power forecast error is set at 4.8, which has the same mean and standard deviation as the normal distribution in [18]. This new probability density function is similarly divided into seven probability intervals, and the median, range, and probability of each interval are shown in Table 3.

Table 3: Parameters of seven-interval approximation for probability distribution with kurtosis 4.8.

Interval number	Median ($\times\sigma_{W,t}$)	Range ($\times\sigma_{W,t}$)	Probability
1	−4	[−5, −3]	0.0049
2	−2.35	[−3, −1.7]	0.0401
3	−1.1	[−1.7, −0.5]	0.2264
4	0	[−0.5, 0.5]	0.4572
5	1.1	[0.5, 1.7]	0.2264
6	2.35	[1.7, 3]	0.0401
7	4	[3, 5]	0.0049

a_{l_1} in (3), (4), and (5) and θ_{l_1} in (10) are taken from the median and probability values of each wind power forecast error interval in Table 3, respectively. Figure 7 compares the SR capacity between the normal distribution and the probability distribution with kurtosis 4.8. It can be seen from this figure that the tail region of forecast error will affect the determination of SR and using the normal distribution to model the wind power forecast error will lead to an increase of the probability of SR insufficiency.

5. Conclusions

Combining cost-benefit analysis with an improved multiscenario risk analysis method capable of taking into account the load and wind power forecast errors as well as FOR of generators, a novel SCUC model with consideration of wind power spillage is proposed in this paper to determine the optimal amount of SR.

In order to consider wind power spillage and the nonnormal distribution of wind power forecast error in system EENS calculation, based on multistep modeling of net demand, the single discretization of net demand forecast error in [20] is extended into the respective discretization of wind power and load forecast errors. From the results of simulation studies, in cases where load and significant wind power

generation are negatively correlated, this model can curtail wind power to maximize the overall economic efficiency of system operation, so that the optimal economic value of wind power and the optimal quantification of SR are achieved. Furthermore, case studies show that the tail region of wind power forecast error will affect the determination of SR and using the normal distribution to model the wind power forecast error may lead to an increase of the probability of SR insufficiency.

Appendix

The fuel cost $c_i(u_i^t, p_i^t)$ of generator i in objective function can be linearized to

$$\begin{aligned} c_i\left(u_i^t, p_i^t\right) &= \left(\sum_{k=1}^{\mathrm{NK}} c_{k,i} p_{k,i}^t + c_{\min,i} u_i^t\right) \\ p_i^t &= u_i^t p_i^{\min} + \sum_{k=1}^{\mathrm{NK}} p_{k,i}^t, \end{aligned} \tag{A.1}$$

where $c_{k,i}$ and $c_{\min,i}$ are cost slope of segment k and minimum fuel cost, respectively, of generator i and $c_{k,i}$ meets $c_{1,i} \le c_{2,i} \le \cdots \le c_{\mathrm{NK},i}$; $p_{k,i}^t$ is the power output of generator i in segment k during period t.

The start-up cost $c_{\mathrm{su},i} u_i^t (1 - u_i^{t-1})$ of generator i in objective function can be linearized to

$$\begin{aligned} c_{\mathrm{su},i} u_i^t \left(1 - u_i^{t-1}\right) &= c_{\mathrm{su},i}\left(u_i^t - x_i^t\right) \\ x_i^t &\le u_i^t \\ x_i^t &\le u_i^{t-1} \\ x_i^t &\ge u_i^t + u_i^{t-1} - 1, \end{aligned} \tag{A.2}$$

where x_i^t is an auxiliary binary variable.

The upper and lower limits (25) for the power output of generators can be linearized to

$$\begin{aligned} 0 &\le p_{1,i}^t \le u_i^t \left(p_{g,1,i} - p_i^{\min}\right) \\ 0 &\le p_{2,i}^t \le u_i^t \left(p_{g,2,i} - p_{g,1,i}\right) \\ &\vdots \\ 0 &\le p_{\mathrm{NK},i}^t \le u_i^t \left(p_i^{\max} - p_{g,(\mathrm{NK}-1),i}\right), \end{aligned} \tag{A.3}$$

where $p_i^{\min}, p_{g,1,i}, p_{g,2,i}, \ldots, p_{g,(\mathrm{NK}-1),i}$ and $p_i^{\max}$ are the NK power points, respectively, of linearized power output interval $[p_i^{\min}, p_i^{\max}]$ of generator i.

The ramp-rate limits (26) of generators can be linearized to

$$p_i^t - p_i^{t-1} \le \left(1 - s_i^t\right) r_u^i + s_i^t p_i^{\min} \tag{A.4}$$

$$p_i^{t-1} - p_i^t \le \left(1 - d_i^t\right) r_d^i + d_i^t p_i^{\min} \tag{A.5}$$

$$s_i^t - d_i^t = u_i^t - u_i^{t-1} \tag{A.6}$$

$$s_i^t + d_i^t \le 1, \tag{A.7}$$

where the binary variables s_i^t and d_i^t are introduced to judge whether the generator i is in the start-up or shutdown process during period t, respectively.

The minimum up- and down-time constraints (27) of generators can be linearized to

$$\begin{aligned} &u_i^m = 1 \\ &\qquad \forall m \in \left[1, \ldots, T_{i,\min}^{\mathrm{up}} - T_{i0}\right],\ T_{i,\min}^{\mathrm{off}} > T_{i0} > 0 \\ &\qquad u_i^t - u_i^{t-1} \le u_i^{t+1} \\ &\qquad u_i^t - u_i^{t-1} \le u_i^{t+2} \\ &\qquad \vdots \\ &\qquad u_i^t - u_i^{t-1} \le u_i^{\min\{t+T_{i,\min}^{\mathrm{up}}-1,\mathrm{NT}\}} \\ &\qquad\qquad \forall t = 2, 3, \ldots, \mathrm{NT} \\ &u_i^m = 0 \\ &\qquad \forall m \in \left[1, \ldots, T_{i,\min}^{\mathrm{off}} + T_{i0}\right],\ -T_{i,\min}^{\mathrm{off}} < T_{i0} < 0 \\ &\qquad u_i^{t-1} - u_i^t \le 1 - u_i^{t+1} \\ &\qquad u_i^{t-1} - u_i^t \le 1 - u_i^{t+2} \\ &\qquad \vdots \\ &\qquad u_i^{t-1} - u_i^t \le 1 - u_i^{\min\{t+T_{i,\min}^{\mathrm{off}}-1,\mathrm{NT}\}} \\ &\qquad\qquad \forall t = 2, 3, \ldots, \mathrm{NT}, \end{aligned} \tag{A.8}$$

where T_{i0} denotes the number of periods in which generator i was committed or decommitted, up to $t = 0$ depending on the sign.

Nomenclature

u_i^t: Binary variable denoting the on/off schedule of generator i during period t
p_i^t: Power output of generator i during period t
r_i^t: Spinning reserve amount of generator i during period t
μ_s^t: Deficient or redundant spinning reserve amount of other generators in accordance with the outage generator i under scenario s
μ_{s,l_1}^t: System forecast error caused by the uncertainties of generators and wind power forecast error

s_W^t: Amount of wind power spillage during period t
W_f^t: Forecast value of wind power during period t
L_f^t: Forecast value of load during period t
μ_W^t, σ_W^t: Mean and standard deviation of wind power forecast error
μ_L^t, σ_L^t: Mean and standard deviation of load forecast error
a_{l_1}, θ_{l_1}: Value and probability of wind power forecast error in interval l_1
θ_{l_2}: Probability of load forecast error in interval l_2
P_i^t: Probability of all scheduled generators available except generator i
r_u^i, r_d^i: Ramp-up and ramp-down rates of generator i in MW/h
$T_{i,\min}^{\text{on}}$, $T_{i,\min}^{\text{off}}$: Minimum up and down time of generator i
$T_{i,t-1}^{\text{on}}$, $T_{i,t-1}^{\text{off}}$: Up and down time which have been accumulated up to period $t-1$
$p_{g,k}^t$: Power output of conventional generators connected to bus k during period t
$p_{w,k}^t$, $p_{\text{sw},k}^t$: Power output of wind farm connected to bus k and the corresponding amount of wind power spillage during period t
$p_{d,k}^t$: Load at bus k during period t
X_{kj}: Reactance of the transmission line kj
δ_k^t: Phase angle of voltage at bus k
$p_{kj}^{\max}$: Capacity limit of line kj
$p_i^{\max}$, $p_i^{\min}$: Maximum and minimum power output of generator i
U_i: Unavailability or forced outage rate of generator i
$c_{\text{su},i}$: Start-up cost coefficient of generator i
$c_{r,i}$: Spinning reserve cost coefficient of generator i
M_C^t, M_D^t: Total amount of carbon emission and the carbon emission credit of power systems during period t
K_{CDM}: Clean Development Mechanism transaction price
α_i, β_i, γ_i, ξ_i and λ_i: Carbon emission coefficients of thermal generator i
$F_{c,i}$: Equivalent carbon emission factor of fuel for generator i
V_S: Unit penalty cost of wind power spillage in \$/MWh
K_F: Price of each ton of standard coal
NT: Number of time periods in the scheduling horizon
NL: Number of intervals of discrete wind power or load forecast error
SR: Spinning reserve
UC: Unit commitment
SCUC: Security-constrained unit commitment
VOLL: Value of lost load
EENS: Expected energy not served
LOLP: Loss of load probability
FOR: Forced outage rate
MILP: Mixed integer linear programming
ECLS: Expected cost of load shedding
GC: Generation cost
PC: Penalty cost
CC: Carbon emission cost
CDM: Clean Development Mechanism.

Conflicts of Interest

The authors declare that there are no conflicts of interest regarding the publication of this paper.

Acknowledgments

The work described in this paper was supported by the Project Supported by State Grid Corporation of China (no. 5210EF150010) and Jiangsu Province Key Technologies R&D Program (BE2014023).

References

[1] P. B. Eriksen, T. Ackermann, H. Abildgaard, P. Smith, W. Winter, and J. M. R. Garcia, "System operation with high wind penetration," *IEEE Power and Energy Magazine*, vol. 3, no. 6, pp. 65–74, 2005.

[2] J. Kabouris and F. D. Kanellos, "Impacts of large-scale wind penetration on designing and operation of electric power systems," *IEEE Transactions on Sustainable Energy*, vol. 1, no. 2, pp. 107–114, 2010.

[3] D. Liu, Y. Huang, W. Wang, and J. Guo, "Analysis on provincial system available capability of accommodating wind power considering peak load dispatch and transmission constraints," *Automation of Electric Power Systems*, vol. 35, no. 22, pp. 77–81, 2011.

[4] G. Dany, "Power reserve in interconnected systems with high wind power production," in *Proceedings of the IEEE Porto Power Tech Conference 2001*, Porto, Portugal, September 2001.

[5] M. H. Albadi and E. F. El-Saadany, "Comparative study on impacts of wind profiles on thermal units scheduling costs," *IET Renewable Power Generation*, vol. 5, no. 1, pp. 26–35, 2011.

[6] M. A. Ortega-Vazquez and D. S. Kirschen, "Assessing the impact of wind power generation on operating costs," *IEEE Transactions on Smart Grid*, vol. 1, no. 3, pp. 295–301, 2010.

[7] X. S. Wu, B. H. Zhang, X. M. Yuan et al., "Solving unit commitment problems in power systems with wind farms using advanced quantum-inspired binary PSO," *Proceedings of the CSEE*, vol. 33, no. 4, pp. 45–52, 2013 (Chinese).

[8] C. Wang, Y. Qiao, and Z. Lu, "A method for determination of spinning reserve in wind-thermal power systems considering wind power benefits," *Automation of Electric Power Systems*, vol. 36, no. 4, pp. 16–21, 2012.

[9] K. Methaprayoon, C. Yingvivatanapong, W.-J. Lee, and J. R. Liao, "An integration of ANN wind power estimation into unit commitment considering the forecasting uncertainty," *IEEE Transactions on Industry Applications*, vol. 43, no. 6, pp. 1441–1448, 2007.

[10] J. Ge, F. Wang, and L. Z. Zhang, "Spinning reserve model in the wind power integrated power system," *Automation of Electric Power Systems*, vol. 34, no. 6, pp. 32–36, 2010 (Chinese).

[11] N. Menemenlis, M. Huneault, and A. Robitaille, "Computation of dynamic operating balancing reserve for wind power integration for the time-horizon 1–48 hours," *IEEE Transactions on Sustainable Energy*, vol. 3, no. 4, pp. 692–702, 2012.

[12] W. Zhou, H. Sun, H. Gu, Q. Ma, and X. Chen, "Dynamic economic dispatch of wind integrated power systems based on risk reserve constraints," *Proceedings of the Chinese Society of Electrical Engineering*, vol. 32, no. 1, pp. 47–55, 2012.

[13] M. A. Matos and R. J. Bessa, "Setting the operating reserve using probabilistic wind power forecasts," *IEEE Transactions on Power Systems*, vol. 26, no. 2, pp. 594–603, 2011.

[14] F. Bouffard and F. D. Galiana, "Stochastic security for operations planning with significant wind power generation," *IEEE Transactions on Power Systems*, vol. 23, no. 2, pp. 306–316, 2008.

[15] J. M. Morales, A. J. Conejo, and J. Pérez-Ruiz, "Economic valuation of reserves in power systems with high penetration of wind power," *IEEE Transactions on Power Systems*, vol. 24, no. 2, pp. 900–910, 2009.

[16] A. Tuohy and M. O'Malley, "Pumped storage in systems with very high wind penetration," *Energy Policy*, vol. 39, no. 4, pp. 1965–1974, 2011.

[17] T.-Y. Lee, "Optimal spinning reserve for a wind-thermal power system using EIPSO," *IEEE Transactions on Power Systems*, vol. 22, no. 4, pp. 1612–1621, 2007.

[18] M. A. Ortega-Vazquez, *Optimizing the Spinning Reserve Requirements*, University of Manchester, Manchester, UK, 2006.

[19] P. Su, T. Q. Liu, and X. Y. Li, "Determination of optimal spinning reserve of power grid containing wind," *Power System Technology*, vol. 34, no. 12, pp. 158–162, 2010 (Chinese).

[20] G. Liu and K. Tomsovic, "Quantifying spinning reserve in systems with significant wind power penetration," *IEEE Transactions on Power Systems*, vol. 27, no. 4, pp. 2385–2393, 2012.

[21] C. Monteiro, R. Bessa, V. Miranda et al., *Wind Power Forecasting: State-of-the-Art 2009*, Argonne National Laboratory (ANL), 2009.

[22] R. Billinton and R. N. Allan, *Reliability Evaluation of Power Systems*, Plenum Press, New York, NY, USA, 2nd edition, 1996.

[23] J. A. Gubner, *Probability and random processes for electrical and computer engineers*, Cambridge University Press, Cambridge, 2006.

[24] K. K. Kariuki and R. N. Allan, "Evaluation of reliability worth and value of lost load," *IEE Proceedings—Generation, Transmission and Distribution*, vol. 143, no. 2, pp. 171–180, 1996.

[25] S. Lu, Y. Wu, S. Lou, and X. Yin, "A model for optimizing spinning reserve requirement of power system under low-carbon economy," *IEEE Transactions on Sustainable Energy*, vol. 5, no. 4, pp. 1048–1055, 2014.

[26] H. Heitsch and W. Römisch, "Scenario reduction algorithms in stochastic programming," *Computational Optimization and Applications*, vol. 24, no. 2-3, pp. 187–206, 2003.

[27] J. R. Birge and F. Louveaux, *Introduction to Stochastic Programming*, Springer Series in Operations Research, Springer, New York, NY, USA, 1997.

[28] M. A. Ortega-Vazquez, D. S. Kirschen, and D. Pudjianto, "Optimising the scheduling of spinning reserve considering the cost of interruptions," *IEE Proceedings: Generation, Transmission and Distribution*, vol. 153, no. 5, pp. 570–575, 2006.